Plasma Science and Technology

PAPER

Study on characteristics of acoustic signals generated by different DC discharge modes

To cite this article: Zilan XIONG *et al* 2023 *Plasma Sci. Technol.* **25** 055404

Plasma Sci. Technol. **25** (2023) 055404 (8pp) https://doi.org/10.1088/2058-6272/acac04

Study on characteristics of acoustic signals generated by different DC discharge modes

Zilan XIONG (熊紫兰)*, Yuqi WANG (王渝淇) and Mengqi LI (李孟琦)

State Key Laboratory of Advanced Electromagnetic Engineering and Technology, Huazhong University of Science and Technology, Wuhan 430000, People's Republic of China

E-mail: zilanxiong@hust.edu.cn

Received 28 October 2022, revised 13 December 2022
Accepted for publication 15 December 2022
Published 21 February 2023

Abstract

Acoustic signals contain rich discharge information. In this study, the acoustic signal characteristics of transient glow, spark, and glow discharges generated through DC pin–pin discharge were investigated. The signals were analyzed in the time, frequency, and time–frequency domains, and the correlation between the electric and the acoustic signal was studied statistically. The results show that glow discharge does not produce measurable sound signals. For the other modes, with a decrease in the discharge gap, the amplitude of the acoustic signal increases sharply with mode transformation, the short-time average energy becomes higher, and the frequency components are more abundant. Meanwhile, the current pulse and sound pressure pulse have a one-to-one relationship in the transient glow and spark regimes, and they are positively correlated in amplitude. A brief theoretical analysis of the mechanism of plasma sound and the trends of signals in different modes is presented. Essentially, the change in the discharge energy is closely related to the sound generation of the plasma.

Keywords: low-temperature plasma, DC discharge, discharging modes, acoustic signal, sound generation

(Some figures may appear in colour only in the online journal)

1. Introduction

In recent years, air plasma produced by discharge at atmospheric pressure has been widely applied in many fields, such as material processing [1], biomedicine [2], and plasma-assisted combustion [3], which has attracted enormous attention. Gas discharge at atmospheric pressure exists in many forms, including glow, spark, and corona discharges [4–6]. Optical, electromagnetic, acoustic, and other signals are always generated during the discharge process. Plasma signals in different regimes are different, and they carry a large amount of information.

Many studies have reported the electrical, optical, chemical, and other characteristics of plasma for different regimes. Images of some discharge modes in different experimental configurations have been presented [4–8], and the discharge modes mainly include corona, spark, glow, and diffuse discharges, as well as some transition states. In recent decades, most studies have focused on the mechanism of mode transition between different modes through electrical measurements and optical emission studies [6, 9–11]. Moreover, several studies on each mode have been conducted from various perspectives. Among these modes, coronas exist in various forms in ambient air, including burst pulse coronas, streamer coronas, and glow coronas [12]. A number of detailed studies on the electrical analysis [13], plasma chemistry [14], and discharge mechanism [15–17] of coronas in various discharge configurations have been reported. Similar studies have also been conducted on the glow [18–21], spark [22–24], and diffuse [8] regimes. In addition to the well-known modes mentioned above, the transient glow mode in DC discharges has also been studied [6]. The discharge current and gas temperature in this mode are much lower than those in the spark discharge but much higher than those in the positive corona, and its appearance confirms that it is a glow-like mode. Additionally, the optical emission spectroscopy for different types of plasma has been studied in detail. It provides the measurement and calculation of many types of information, including the types of active species, OH radical concentration, gas temperature, plasma size, and electron number density, which helps to better

* Author to whom any correspondence should be addressed.

understand the plasma chemistry [15, 25, 26]. Furthermore, many scholars have established mathematical models or numerical simulations for further analysis [27–30].

Apart from the electrical, optical, and physical characteristics generated by plasma, acoustic signals are also typical during gas discharge. In recent decades, research on the acoustic signals of gas discharge has focused on the audible noise of corona discharges generated on high-voltage transmission lines. The sound pressure waveforms have been measured and analyzed at different discharge parameters by a series of experiments, and detailed characteristics of both the time and frequency domains have been well summarized [31–33]. Meanwhile, aiming at investigating the mechanism of audible noise caused by corona discharge, a numerical model based on the fluid equations of the species in the air has been established and validated using experiment data [34]. Hitherto, however, no research on the characteristics and mechanism of plasma acoustic signals in different discharge modes in DC discharge has been reported.

In this study, we measured and analyzed the acoustic signals of different DC discharge modes in the time, frequency, and time–frequency domains and studied the correlation between the electric and the acoustic signal. Further, the mechanism of the plasma sound was briefly analyzed based on experimental results and existing research.

2. Experimental setup and methods

2.1. Experimental setup

A diagram of the experimental setup is sketched in figure 1. A pin–pin plasma device driven by a positive DC power supply (Spellman SL30PN300) was used. The applied voltage was fixed at 14 kV. Two stainless needles, the powered and grounded electrodes, were fixed on the slide rail; therefore, the gap between the two needle tips could be adjusted from 0 to 12 cm for the discharge mode transformation. A ballast resistor R of 10 MΩ was connected in series in the circuit.

The applied voltage V_a and discharge voltage V_d were measured by high-voltage probes (Tektronix P6015A). A current probe (Pearson 2877) was used to measure the pulse current I, and the voltage V_r was measured by a differential probe (Tektronix P5200A) across a 930 Ω resistor r. Subsequently, the direct current in the circuit was calculated according to $I = V_r/r$. The discharge images were captured using a digital camera (NIKON D750) with an exposure time of 0.4 s. Acoustic signals were recorded using a microphone (BSWA MPA401) with a bandwidth of 10 to 70 kHz and a sensitivity of 5 mV/Pa, situated at the same elevation as the discharge spot at a height of 10 cm.

2.2. Methods

Generally, the waveform of the collected acoustic signal exhibits burrs and electromagnetic interference. For a more accurate analysis, a median filter was first applied to remove the glitches from the waveform. The basic principle of median filtering is to replace the value in the processed signal with the median value of each point in a neighborhood. This eliminates isolated noise points without destroying signal characteristics. Samples of the background noise and denoising results are presented in appendix A. The analysis of the acoustic signal in the following sections is based on denoised waveforms.

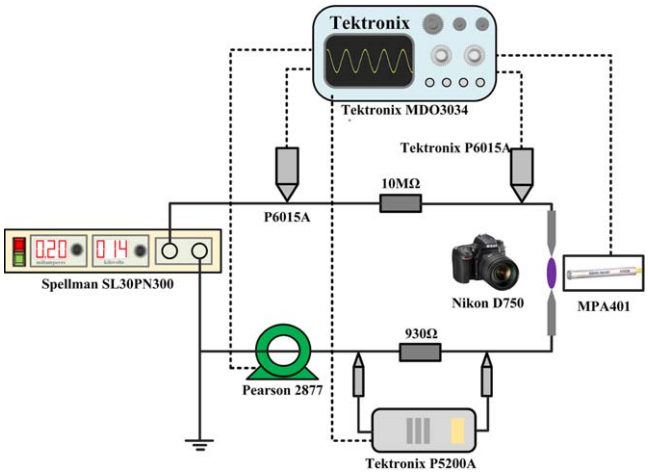

Figure 1. Sketch of experimental setup.

Since the acoustic signal is generated from air vibration, the energy of the plasma acoustic signal varies with time and differs greatly in different discharge modes. The short-time average energy E_n is a common time-domain feature used to describe the change in the plasma acoustic signal, which at time n is defined as [35]

$$E_n = \sum_{m=n-(N-1)}^{n} [x(m)w(n-m)]^2, \tag{1}$$

where $x(m)$ represents the acoustic signal, $w(n-m)$ the window function, and N the window length.

For acoustic signals, more relevant information is usually obtained in the frequency domain. Therefore, it is necessary to discuss the spectral characteristics of plasma acoustic signals. Fast Fourier transform (FFT) is a common method of frequency domain analysis, and the FFT definition for a discrete signal is as follows:

$$X(k) = \sum_{n=0}^{N-1} x(n)\mathrm{e}^{-\mathrm{j}\frac{2\pi nk}{N}}, \ 0 \leqslant k \leqslant N-1, \tag{2}$$

where $X(k)$ represents the amplitude estimation of $x(n)$.

However, the frequency domain characteristics cannot provide time information, and the time–frequency diagram generated by short-time Fourier transform (STFT) is commonly used to solve this problem. The calculation method consists of two steps. First, the acoustic signal is divided into frames, then FFT is applied to each frame, and finally, a two-dimensional diagram is obtained. This diagram takes time as the abscissa and frequency as the ordinate, and the points in the diagram represent the power spectrum estimates $P(k)$ of the acoustic signal, which are calculated by

$$P(k) = 10 \times \log_{10}\left(|X(k)|^2 \times \frac{1}{nfft}\right), \tag{3}$$

where $nfft$ is the number of signal points of each frame.

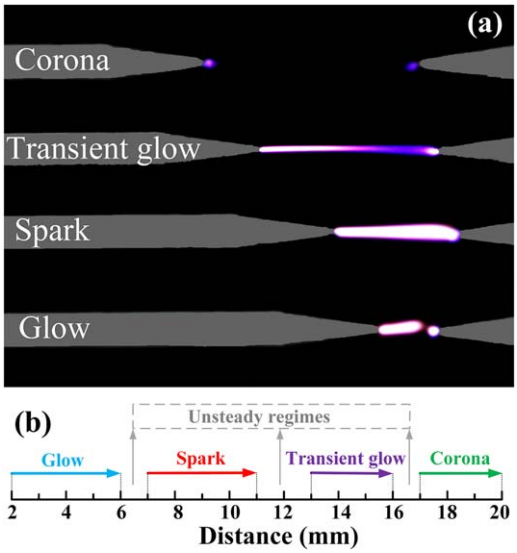

Figure 2. Image and division map of the different discharge modes.

3. Results

3.1. Discharging modes

According to the existing literature, different discharging modes were divided based on the appearance [4–6]. The typical discharge images of the four modes and a division map are presented in figure 2. As illustrated in figure 2(a), the powered electrode is on the left side whereas the grounded electrode is on the right. A corona discharge appears at 20 mm. There is a weak spherical plasma around the two needle tips, but the air gap does not break down completely. In addition, when the discharge gap decreases in this mode, the plasma area and brightness increase. At approximately 16 mm, the discharge mode changes to a transient glow discharge, which mainly comprises a small bright area around the cathode and a bright plasma column near the anode. A slightly dark area can be observed between the two discharge areas. As the discharge distance reduces to approximately 11 mm, the air gap is completely broken down, and the entire discharge area produces strong white light. This discharge state is recognized as spark discharge. The final mode is the glow discharge, which occurs at less than 6 mm. It can be observed that this discharge mode includes a positive column, Faraday dark space, and negative glow.

In this experiment, this type of corona was regarded as a glow corona [12]. It operates quietly, that is to say, no obvious audible sound can be directly heard during discharge. Moreover, the waveform of the acoustic signal in this mode appears irregular, and the amplitude is so small that it is difficult to extract from noise. For further analysis, a more sophisticated microphone for low sound pressures is required. Consequently, the corona mode was not analyzed in this study.

3.2. Characteristics of electrical and acoustic signals under transient glow discharge

Figure 3 shows the electric and acoustic signals of the transient glow discharge at a gap distance of 14 mm. The discharge signal of the transient glow mode appears periodically, and its

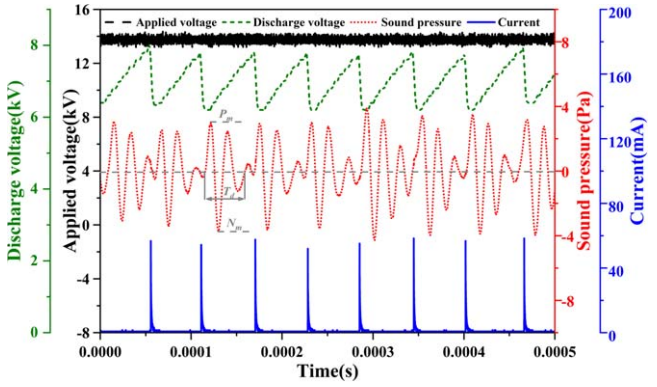

Figure 3. Electric and acoustic signal waveforms of transient glow mode.

repetition frequency is approximately 17 kHz in approximately eight discharge cycles in 500 μs. The discharge voltage lasts for approximately 52 μs, and the drop voltage increases to approximately 1.65 kV. The current exhibits a similar trend. The peak current increases to approximately 60 mA, and the full width at half maximum (FWHM) is approximately 50 ns. During the experiment, a sharp sibilant sound can be heard. The time-domain waveform of the acoustic signal consists of a series of random sound pressure pulses with bipolar properties. Closely examining a single pulse, the first positive amplitude (P_m) is approximately 3 Pa whereas the first negative amplitude (N_m) is approximately −3.5 Pa. We defined the duration of the first two obvious cycles in the sound waveform as its period, T_d, which was approximately 40 μs in this operated mode.

Figure 4(a) shows the calculation for short-time average energy. The amplitude is large but the range of variation is relatively stable. The frequency spectrum of the measured acoustic signal is presented in figure 4(b). It is evident that the transient glow discharge induces many high-frequency components, mainly comprising approximately 17, 35, 52, and 70 kHz. These spectral components—roughly multiples of 17 kHz—are included both within and outside the auditory response range of the human ear. In view of the STFT graph, owing to the smooth operation, four distinct frequency bands can be observed, which is consistent with the FFT result. The power of the spectral components in the audible range is approximately −17 dB in amplitude, which is lower than that of other high-frequency components; for example, the value of power spectrum around 52 kHz is approximately −4 dB.

3.3. Characteristics of electric and acoustic signals under spark discharge

As shown in figure 5, compared with the transient glow discharge, the discharge frequency of the spark mode is lower, maintaining a repetition of approximately 8 kHz for a gap distance of 8 mm. The shape of the discharge voltage resembles a sawtooth wave. The peak-to-peak value is very high, approximately 7.7 kV, and the period is approximately 147 μs. Moreover, I_{peak} increases to approximately 1.9 A and the FWHM is approximately 50 ns. The spark discharge produces a buzzing sound mixed with a crackling, loud, and harsh sound. The acoustic waveforms are also bipolar pulses

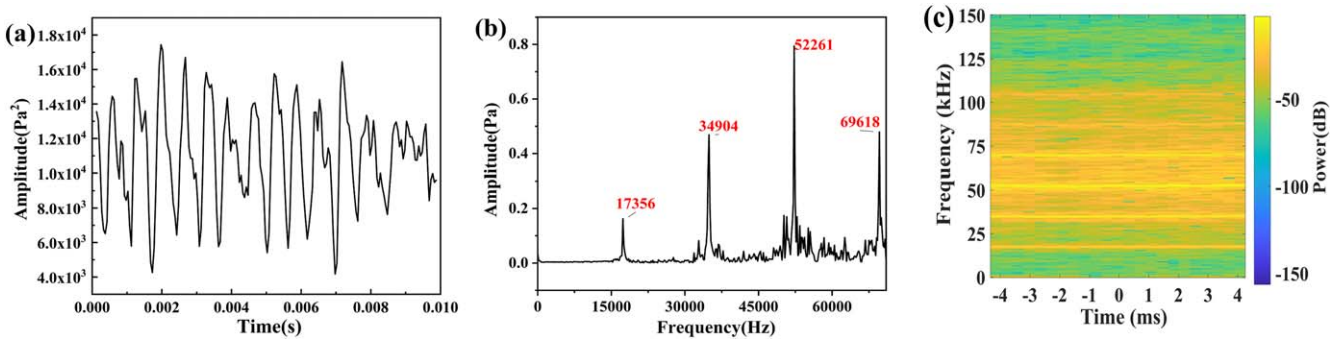

Figure 4. Analysis of acoustic signal under transient glow discharge. (a) Short-time average energy, (b) frequency-domain curves, and (c) STFT of acoustic signal.

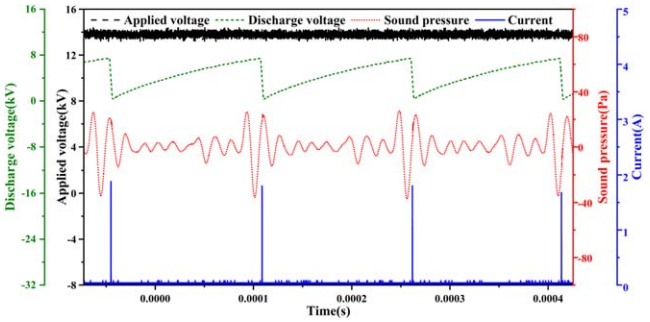

Figure 5. Electric and acoustic signal waveforms of spark mode.

with a shape similar to that in the transient glow mode. The amplitude of the sound pressure is much larger than those in other modes, in which P_m is approximately 20 Pa and N_m is approximately −31 Pa. The sound pulse lasts for approximately 38 μs, which does not change much compared to that of the transient glow mode. Compared to other modes, spark discharge is relatively more unstable; consequently, the parameters vary significantly per discharge cycle.

As shown in figure 6(a), the amplitude of the short-time average energy considerably exceeds that of the transient glow mode several hundred times over, with a wider range of variation. From the frequency spectrum shown in figure 6(b), despite the lower discharge frequency, it can be observed that the spark discharge contains more abundant frequency components compared to the other regimes. Further, the basic frequency shifts from 17 kHz to approximately 7 kHz, and all wave crests essentially appear at multiples of basic frequency. As shown in the STFT graph, spark discharge operates in a stable state in 10 ms, and more frequency bands can be observed. Furthermore, the number of frequency bands detected in the spark regime within the auditory response range of the human ear surpasses that in the transient glow regime. The power spectrum of these frequency components is approximately −10 dB, which is significantly lower than that of the components outside the audible range (approximately 10 dB).

3.4. Characteristics of electric and acoustic signals under glow discharge

When the discharge distance is reduced to less than 6 mm, the spark discharge changes into the glow discharge mode. As shown in figure 7, in this mode, the discharge current and voltage are both in the DC state, where the voltage is approximately 2.8 kV and the current is approximately 1 mA. Meanwhile, it can be observed that the amplitude of the filtered acoustic signal has almost no fluctuation; that is, no sound wave could be measured, which corresponds to the phenomenon whereby no sound is heard during glow discharge in the experiment. As shown in figure 8(a), the short-time average energy is small. Further, as shown in the FFT and STFT graphs, the spectrum mainly consists of a DC component, and the intensity is approximately −35 dB.

4. Discussion

4.1. Correlation between electric and acoustic signals

The relationship between electric and acoustic signals is important for understanding the mechanism of plasma sound; hence, they are measured at different discharge distances to analyze the relationship between parameters. Since the frequency spectrum of the glow regime mainly consists of a DC component, and given the signal of the corona discharge is weak and irregular, only the transient glow and spark discharge modes are discussed in this section. In this study, since we mainly focus on the characteristics of acoustic signals in different discharge modes, the typical FFT results of current signals in different discharge modes are supplemented in appendix B.

4.1.1 Correlation of frequencies in frequency domain. From the above experimental results, it can be clearly noted that there is one-to-one correspondence between the current pulse and the sound wave in the transient glow and spark regimes. This leads us to explore their correlation in the frequency domain. The spectral components of the two signals at different gap distances under the transient glow and spark discharge modes are summarized in figure 9. Given the frequency response of the microphone ranges from 10 to 70 kHz, we focus on the frequency components in this range. In the case of the transient glow mode, with a reduction in the distance, the number of frequency components gradually increases, whereas the trend is reversed in the spark mode. Interestingly, the frequency components presented are almost identical for both the

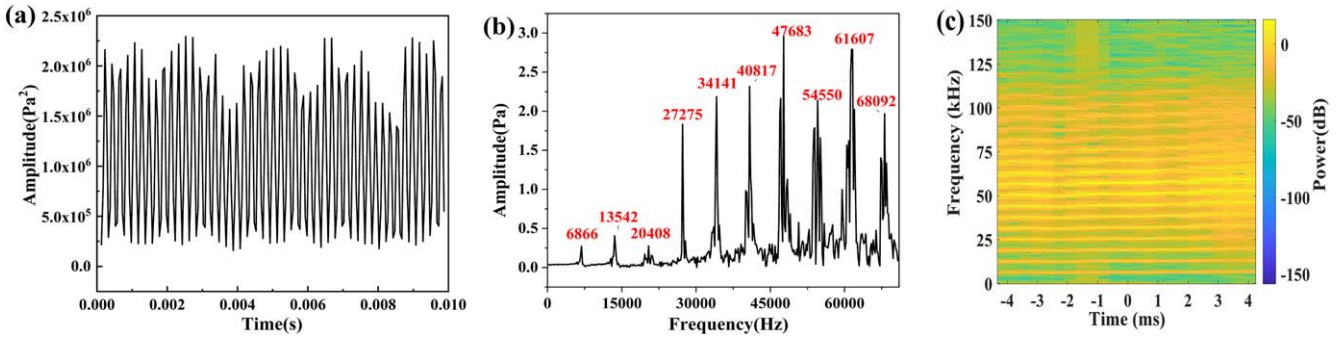

Figure 6. Analysis of acoustic signal under spark discharge. (a) Short-time average energy, (b) frequency-domain curves, and (c) STFT of acoustic signal.

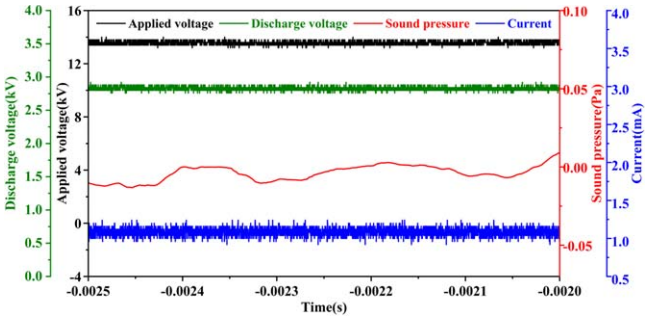

Figure 7. Electric and acoustic signal waveforms of glow mode.

acoustic and current signals in these two modes. This implies that the frequency components of the acoustic signal are induced by those of the current signal, and there is a strong correlation between them in the frequency domain.

4.1.2. Correlation of waveform parameters in time domain. Notably, the acoustic signal is related to the parameters of both voltage and current. However, the results [36] indicate that a stronger correlation exists between acoustic and current signals; therefore, we focused on the parameters of the current. Nevertheless, although the experimental conditions do not change, the waveform is not exactly the same in every period during DC discharge. A statistical method was used to investigate the relationship between the parameters of the current pulse and the corresponding sound pulse during a single period. In this experiment, the gap was adjusted in steps of 1 mm, and ten groups of data were collected—within 10 ms each time—at every discharge distance. The statistical results of the current and acoustic signals under transient glow and spark modes are listed in table 1, where each parameter is obtained based on the average value of all collected data.

In the transient glow mode, with the reduction in the discharge distance, the repetition frequency first increases and then decreases, whereas both the peak value and FWHM of the current pulse and the average current increase. Likewise, the peaks of the acoustic signal also exhibit an increasing trend, but the period of a sound pulse barely changes. In the case of the spark mode, the variation trend of each parameter differs from that in the transient glow mode. The repetition frequency is much lower and increases with the reduction in the discharge gap. The FWHM exhibits the same trend but increases by a relatively small margin. The peak value of the current increases sharply, but the trend is opposite to that in the transient glow mode. Although the changing trends of the parameters of the current pulse are different, the calculated average current continues to increase as the distance decreases. In terms of the acoustic signal, compared to that in the transient glow mode, the period remains fairly constant, but the peak values of the sound pulse are much larger, and their variation trends are opposite.

Overall, in both discharge modes, it can be seen that the change trend only shows a positive correlation between the peaks of the current signal and the acoustic signal. Consequently, it is assumed that the main factor affecting the change in sound pressure is the peak value of current.

4.2. Brief theoretical analysis of the mechanism of plasma sound

In this study, we investigated the relationship between electric and acoustic signals in the transient glow and spark discharge modes in DC discharge. Sound is caused by atmospheric vibrations and is a manifestation of energy change. It can be inferred that the energy in the acoustic signal originates mainly from the energy injected by the current pulse.

Combining the above analysis and the existing research findings, a simple hypothesis of the mechanism of generation of acoustic signals by gas discharge can be summarized as follows. The air is broken down owing to the injection of discharge energy. Subsequently, via electron-impact and dissociative quenching reactions, a large amount of heat is produced in tens of nanoseconds [37, 38]. The gas heating around the discharge area continues, creating a pressure gradient. This leads to hydrodynamic expansion of air, and thus the number density of neutral molecules decreases with increasing volume. Then, at the end of a discharge cycle, the temperature drops and the air gap gradually recovers. During this process, air pressure oscillates per discharge period, hence the acoustic wave. Consequently, the current pulse corresponds to the sound pressure pulse directly. The positive peak of the acoustic wave corresponds to the expansion of air, and the negative peak corresponds to contraction.

Studies combining experiments and theory have been conducted to explore the mechanism of plasma sound. The theory of the motion of the neutral-gas component in the

Table 1. Measurement results of current and acoustic signals at different distances.

Mode	Distance (mm)	Current signal				Acoustic signal		
		f (kHz)	FWHM (ns)	I_{peak} (A)	I_{avg} (mA)	T_d (μs)	P_m (Pa)	N_m (Pa)
Transient glow	16	12.50	27.90	0.027	0.0093	39.18	0.35	0.49
	15	19.27	36.98	0.052	0.0383	37.59	0.84	1.21
	14	17.47	48.85	0.059	0.0531	40.17	1.62	2.63
	13	15.76	152.89	0.060	0.1450	39.58	2.81	4.39
Spark	11	4.77	40.84	2.38	0.453	39.10	24.43	40.28
	10	6.15	46.61	2.26	0.610	38.77	21.81	33.98
	9	6.24	46.45	2.25	0.620	38.49	20.12	33.62
	8	7.16	49.06	2.03	0.712	38.90	20.43	31.77
	7	8.84	54.51	1.92	0.763	39.94	17.31	26.25

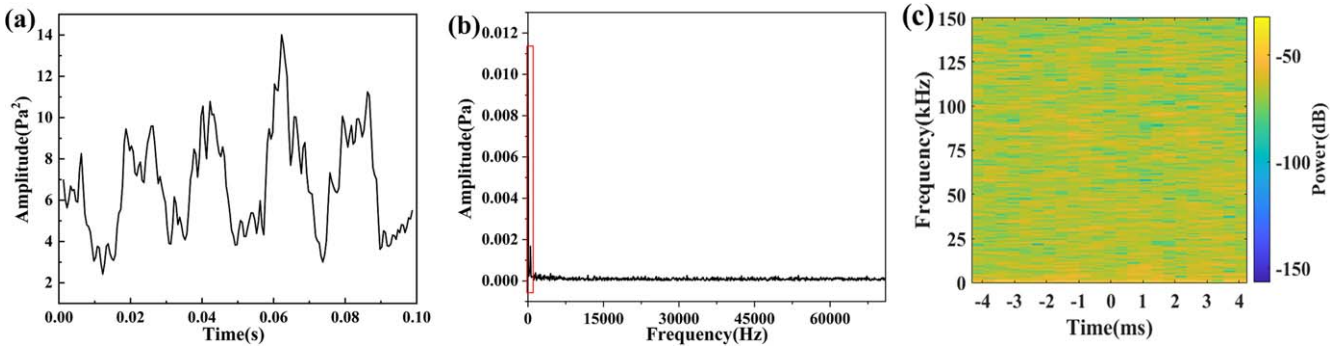

Figure 8. Analysis of acoustic signal under glow discharge. (a) Short-time average energy, (b) frequency-domain curves, and (c) STFT of acoustic signal.

plasma proposed by Ingard is widely accepted [39]. During gas discharge at atmospheric pressure, since the density of charged particles is much smaller than that of neutral components, the acoustic signal in the plasma is mainly caused by changes in the pressure and density of neutral molecules. Based on this assumption, by integrating the mass, momentum, and energy density conservation equations, Ingard [39] obtained the wave equation (4) of the neutral molecules:

$$\frac{1}{c^2}\frac{\partial^2 p}{\partial t^2} - \nabla^2 p = \frac{(\gamma - 1)}{c^2}\frac{\partial H}{\partial t}, \tag{4}$$

where c is the velocity of the sound wave, p denotes the perturbation of the pressure, γ is the ratio of the specific heats of air, and H represents the rate of energy transfer to neutral molecules per unit volume. In this equation, the relatively small mass and momentum source terms have been neglected [40]. Since the mass of the electron is much smaller than that of the ion, H acts as the source term of the acoustic signal, which is mainly obtained from the energy transfer from electrons to neutral molecules in the collision. Moreover, Bastien [40] experimentally confirmed that the energy rate injected into the neutral gas is proportional to the derivative of input electric power at constant pressure, that is, H varies with power W.

It can be observed that the generation of sound is closely related to the change in the electric signal, which has also been confirmed in our experiments. The currents of the transient glow and spark discharge regimes are all in pulse form and thus their discharge energy changes periodically, whereas the glow discharge is a DC discharge and thus its discharge energy does not change. Therefore, no sound was produced during glow discharge, but the acoustic signal could be measured by a microphone in the other modes.

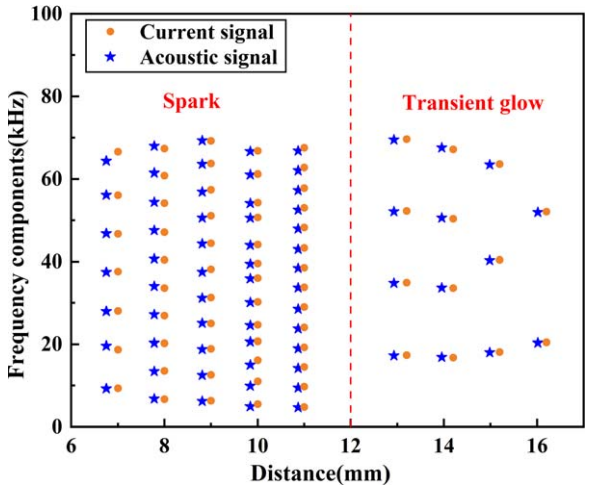

Figure 9. Frequency components at different discharge distances.

Figure 10 shows the derivative of plasma power in the transient glow and spark discharge modes, which can be used to explain the difference in the amplitude of the acoustic signal. For further analysis, a more sophisticated microphone for low sound pressures is required. For transient glow and

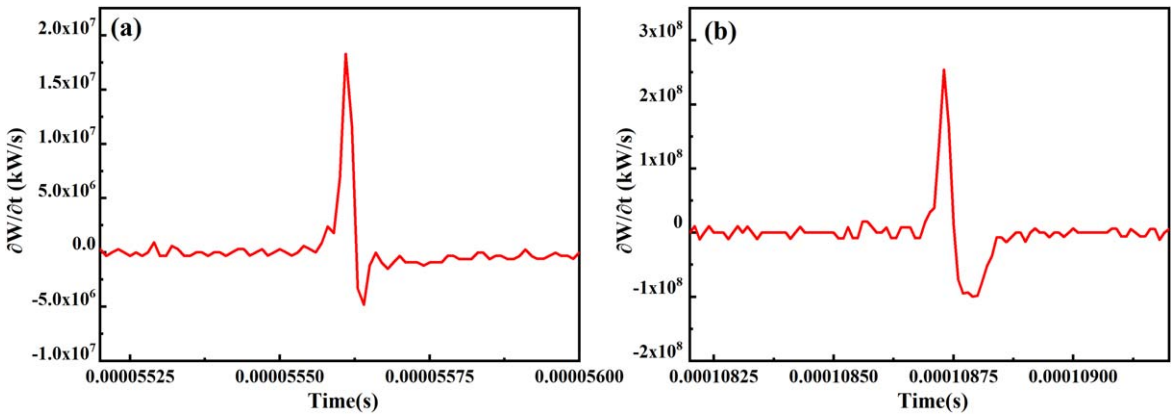

Figure 10. Derivative of plasma power. (a) Transient glow discharge, (b) spark discharge.

spark modes, the waveforms of acoustic signals have similar shape but unequal amplitudes. As shown in figure 10(a) and (b), the reason for the different amplitudes of the acoustic signal is that the value of $\partial W/\partial t$ in the transient glow mode is much smaller than that in the spark discharge mode.

5. Conclusions

In this study, we investigated and compared the electric and acoustic signals of different DC discharge modes. Four discharge modes were obtained by changing the discharge distance, namely corona, transient glow, spark, and glow discharge modes. The electric and acoustic signals in different discharge modes exhibit different characteristics in the time, frequency, and time–frequency domains. This study focused on the latter three discharge modes; all three operated steadily during the measurements. Notably, glow discharge does not produce sound because it is a DC discharge. However, with the decrease in gap, the amplitude and short-time average energy of the acoustic signal increase sharply with mode transformation from transient glow to spark. Considering the frequency domain, the spectral components are more abundant with the reduction in distance. Meanwhile, the current pulse and the sound pressure pulse have a one-to-one relationship in the transient glow and spark modes, and they are positively correlated in amplitude.

In addition, we briefly discussed the mechanism of plasma sound using simple theoretical analysis. The generation of the acoustic signal is closely related to the electric signal, in which the movement of neutral molecules in the discharge gap is caused by the injection of the discharge energy. From the equations of motion of the neutral-gas component, it can be seen that the amplitude of the acoustic signal is positively correlated with the derivative of the power input.

Future work should focus on detailed quantitative analyses and numerical calculations to further understand the differences in the mechanism of plasma sound in different discharge modes.

Acknowledgments

This work is supported by National Natural Science Foundation of China (No. 52177145).

Appendix A

Before discharging, the background noise was first measured, as shown in figure A1(a). The noise mainly originates from

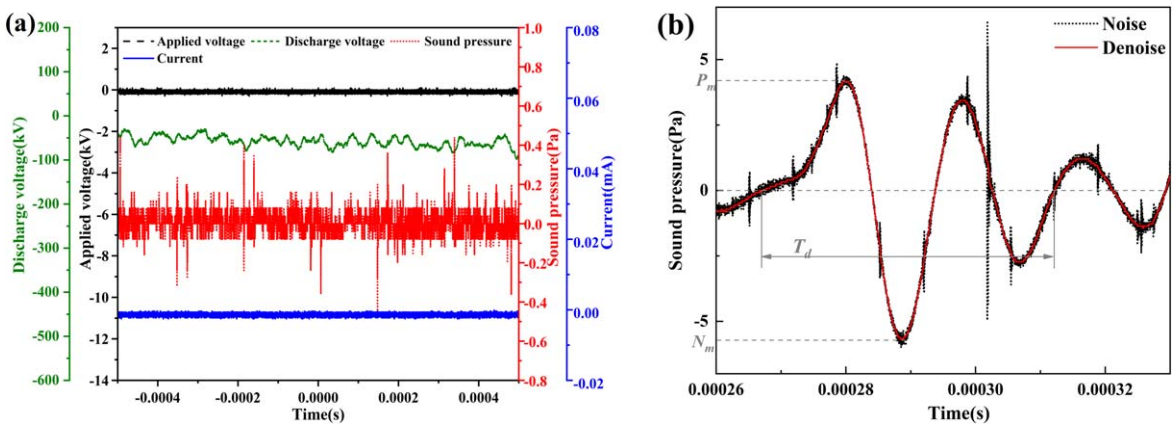

Figure A1. (a) Waveform of background noise, (b) denoising of acoustic signal.

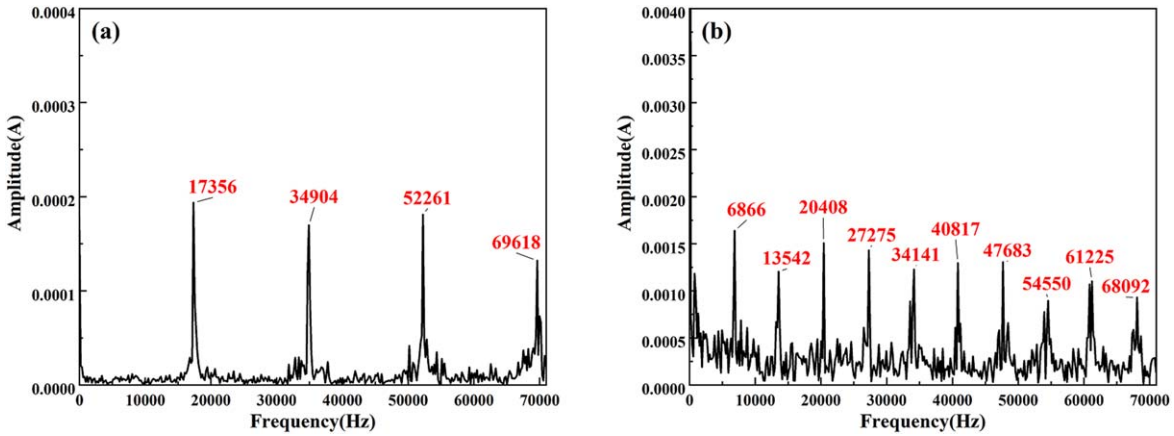

Figure B1. Frequency-domain curves of (a) transient glow mode in 14 mm, (b) spark mode in 8 mm.

the self-noise of the microphone and oscilloscope as well as the environment noise. However, the background noise is minimal and has negligible impact on the measurement of acoustic signals. A median filter was used before analyzing the acoustic signal. It can be seen that the waveform of the acoustic signal is smooth after denoising in figure A1(b).

Appendix B

The typical FFT results of current signal corresponding to each discharge mode in section 3.2 are shown in figure B1. It can clearly be seen that there is one-to-one correspondence between the current and the sound in the frequency domain.

References

[1] Kostov K G *et al* 2014 *Appl. Surf. Sci.* **314** 367
[2] Xiong Z L *et al* 2021 *Plasma Process. Polym.* **18** 2000204
[3] Ju Y G and Sun W T 2015 *Prog. Energy Combust. Sci.* **48** 21
[4] Pai D, Lacoste D and Laux C 2008 Nanosecond repetitively pulsed plasmas in preheated air at atmospheric pressure - the diffuse regime *Proc. 39th Plasmadynamics and Lasers Conf. Seattle* (Washington: AIAA) 2008, 1
[5] Machala Z, Jedlovsky I and Martisovits V 2008 *IEEE Trans. Plasma Sci.* **36** 918
[6] Wu S Q *et al* 2018 *Phys. Plasmas* **25** 123507
[7] Shao T *et al* 2011 *IEEE Trans. Plasma Sci.* **39** 1881
[8] Zhang C *et al* 2011 *IEEE Trans. Plasma Sci.* **39** 2208
[9] Akishev Y *et al* 2001 *J. Phys. D: Appl. Phys.* **34** 2875
[10] Pai D Z, Lacoste D A and Laux C O 2010 *J. Appl. Phys.* **107** 093303
[11] Janda M *et al* 2012 *Plasma Sources Sci. Technol.* **21** 045006
[12] Chang J S, Lawless P A and Yamamoto T 1991 *IEEE Trans. Plasma Sci.* **19** 1152
[13] Dubois D *et al* 2007 *J. Appl. Phys.* **101** 053304
[14] Lowke J J and Morrow R 1994 *Pure Appl. Chem.* **66** 1287
[15] Akishev Y *et al* 2005 *Plasma Sources Sci. Technol.* **14** S18
[16] Zhang C, Shao T and Yan P 2014 *Chin. Sci. Bull.* **59** 1919 (in Chinese)
[17] Morrow R 1997 *J. Phys. D: Appl. Phys.* **30** 3099
[18] Machala Z *et al* 2004 *J. Adv. Oxid. Technol.* **7** 133
[19] Gudmundsson J T and Hecimovic A 2017 *Plasma Sources Sci. Technol.* **26** 123001
[20] Korolev Y D *et al* 2012 *IEEE Trans. Plasma Sci.* **40** 2951
[21] Pai D Z *et al* 2009 *Plasma Sources Sci. Technol.* **18** 045030
[22] Pai D Z, Lacoste D A and Laux C O 2010 *Plasma Sources Sci. Technol.* **19** 065015
[23] Janda M *et al* 2015 *J. Phys. D: Appl. Phys.* **48** 035201
[24] Janda M, Martišovitš V and Machala Z 2011 *Plasma Sources Sci. Technol.* **20** 035015
[25] Bruggeman P *et al* 2008 *J. Phys. D: Appl. Phys.* **41** 215201
[26] Staack D *et al* 2008 *Plasma Sources Sci. Technol.* **17** 025013
[27] Marode E, Bastien F and Bakker M 1979 *J. Appl. Phys.* **50** 140
[28] Naidis G V 2008 *J. Phys. D: Appl. Phys.* **41** 234017
[29] Naidis G V 2009 *Eur. Phys. J. Appl. Phys.* **47** 22803
[30] Tholin F and Bourdon A 2013 *J. Phys. D: Appl. Phys.* **46** 365205
[31] Li X *et al* 2014 Time-domain and frequency-domain characteristics of audible noise from single corona source *Proc. 2014 Int. Conf. on Power System Technology* (Chengdu: IEEE) 2014, 1410
[32] Li X B *et al* 2015 *IEEE Trans. Dielectr. Electr. Insul.* **22** 1314
[33] Li X B *et al* 2018 *IEEE Trans. Plasma Sci.* **46** 3690
[34] Zhang B, Li Z and He J L 2017 *Phys. Plasmas* **24** 103521
[35] Wei W F *et al* 2019 *Proc. Inst. Mech. Eng. Part F J. Rail Rapid Transit* **233** 506
[36] Ren C Y *et al* 2013 *High Voltage Eng.* **39** 2038
[37] Popov I B *et al* 2013 Experimental study and numerical simulation of flow separation control with pulsed nanosecond discharge actuator *Proc. 51st AIAA Aerospace Sciences Meeting including the New Horizons Forum and Aerospace Exposition* (Grapevine: AIAA) 2013, 1
[38] Popov N A 2001 *Plasma Phys. Reports* **27** 886
[39] Ingard U 1966 *Phys. Rev.* **145** 41
[40] Bastien F 1987 *J. Phys. D: Appl. Phys.* **20** 1547